ACS chemical biology

pubs.acs.org/acschemicalbiology

Articles

Orthosteric and Allosteric Dual Targeting of the Nuclear Receptor RORγt with a Bitopic Ligand

Femke A. Meijer,[†] Guido J.M. Oerlemans,[†] and Luc Brunsveld*

Cite This: *ACS Chem. Biol.* 2021, 16, 510–519

Read Online

ACCESS | Metrics & More | Article Recommendations | Supporting Information

ABSTRACT: The RORγt nuclear receptor (NR) is of critical importance for the differentiation and proliferation of T helper 17 (Th17) cells and their production of the pro-inflammatory cytokine IL-17a. Dysregulation of RORγt has been linked to various autoimmune diseases, and small molecule inhibition of RORγt is therefore an attractive strategy to treat these diseases. RORγt is a unique NR in that it contains both a canonical, orthosteric and a second, allosteric ligand binding site in its ligand binding domain (LBD). Hence, dual targeting of both binding pockets constitutes an attractive alternative molecular entry for pharmacological modulation. Here, we report a chemical biology approach to develop a bitopic ligand for the RORγt NR, enabling concomitant engagement of both binding pockets. Three candidate bitopic ligands, **Bit-L15**, **Bit-L9**, and **Bit-L4**, comprising an orthosteric and allosteric RORγt pharmacophore linked via a polyethylene glycol (PEG) linker, were designed, synthesized, and evaluated to examine the influence of linker length on the RORγt binding mode. **Bit-L15** and **Bit-L9** show convincing evidence of concomitant engagement of both RORγt binding pockets, while the shorter **Bit-L4** does not show this evidence, as was anticipated during the ligand design. As the most potent bitopic RORγt ligand, **Bit-L15**, antagonizes RORγt function in a potent manner in both a biochemical and cellular context. Furthermore, **Bit-L15** displays an increased selectivity for RORγt over RORα and PPARγ compared to the purely orthosteric and allosteric parent compounds. Combined, these results highlight potential advantages of bitopic NR modulation over monovalent targeting strategies.

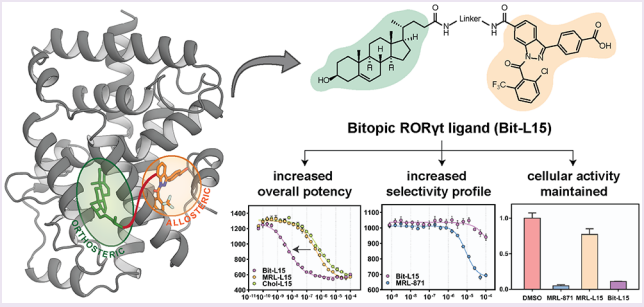

1. INTRODUCTION

The retinoic acid receptor-related orphan receptor γ t (RORγt) is an NR that plays an important regulatory role in the immune system.[1−3] RORγt expression is limited to the lymphoid system, where it is essential for the differentiation of naïve CD4$^+$ T cells into Th17 cells and the production of the pro-inflammatory cytokine IL-17a.[1−3] Elevated IL-17a levels are highly associated with the pathogenesis of autoimmune diseases, including multiple sclerosis, rheumatoid arthritis, and psoriasis.[4−7] Disrupting the Th17/IL-17a pathway could therefore potentially be an effective strategy for the treatment of these diseases.[4] The clinical successes of FDA-approved monoclonal antibodies targeting IL-17a or Th17 cell development have already validated the potential of Th17 pathway inhibition as a successful therapeutic strategy.[8] However, inhibition of RORγt with small molecules might be an attractive alternative strategy to decrease IL-17 production in the treatment of these autoimmune diseases, which has been the focus of many research efforts over the past decades, resulting in the development of several synthetic RORγt inverse agonists.[9−14]

Typically, NR ligands bind to a highly conserved hydrophobic binding pocket, termed orthosteric site, located within the ligand binding domain (LBD) of RORγt.[1,9] RORγt features some level of background transcriptional activity because Helix 12 (H12/AF-2) is already positioned in a conformation that enables coactivator recruitment in the apo form.[15] Regardless, RORγt is responsive to ligand binding with cholesterol (Figure 1) and its derivatives acting as agonists for RORγt,[1,16] stabilizing H12 in an active conformation, resulting in an increased recruitment of coactivators. Conversely, inverse agonist binding destabilizes the active conformation of H12, disrupting the coactivator binding groove and thus decreasing the transcriptional activity. Recently, a novel class of RORγt inverse agonists has been identified, typified by **MRL-871**, which bind to a topographically distinct, allosteric site of the RORγt LBD, formed by helices 3, 4, 11, and reoriented H12 (Figure 1).[17−20] The interactions in this allosteric pocket are predominantly hydrophobic, in addition to the hydrogen bonds between the carboxylic acid moiety of **MRL-871** and the backbone hydrogen atoms of Ala497 and Phe498 as well as the side chain of residue Gln329.[17] These allosteric ligands

Received: December 6, 2020
Accepted: February 8, 2021
Published: February 17, 2021

ACS Publications

© 2021 The Authors. Published by American Chemical Society

https://dx.doi.org/10.1021/acschembio.0c00941
ACS Chem. Biol. 2021, 16, 510–519

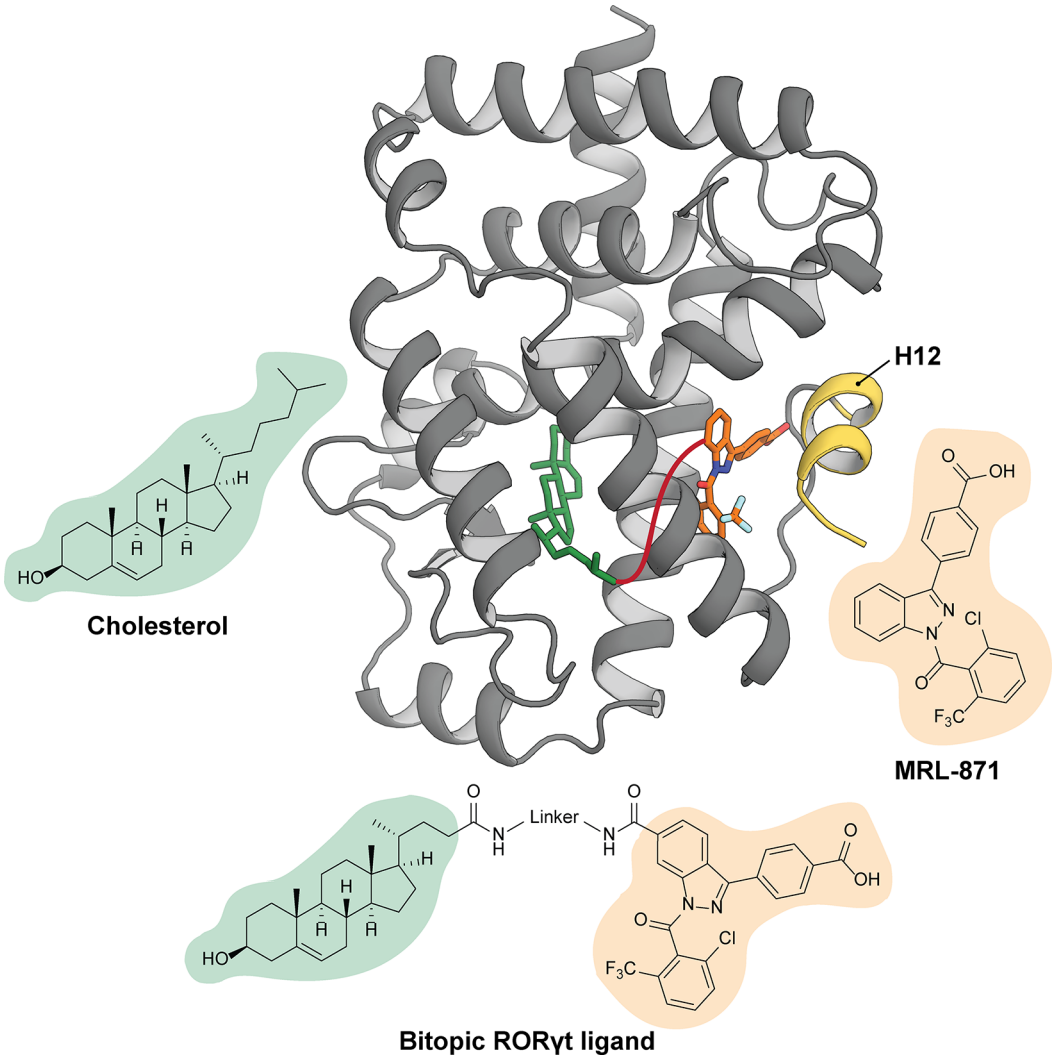

Figure 1. Crystal structure of RORγt with **MRL-871** in the allosteric site (orange sticks) and cholesterol in the orthosteric site (green sticks); H12 is shown in yellow (PDB ID: 6T4I).[24] The chemical structures of the orthosteric agonist cholesterol (green), allosteric inverse agonist **MRL-871** (orange), and the general design of the bitopic RORγt ligand (orthosteric cholesterol pharmacophore in green, allosteric **MRL-871** pharmacophore in orange) are shown as well. The envisioned path of the linker connecting the orthosteric and allosteric pharmacophores is shown as a red line in the crystal structure.

decrease the transcriptional activity of RORγt by repositioning H12 in a conformation incompatible with coactivator binding and thus directly affect the activity of RORγt.[17] Interestingly, these ligands show a high potency (low nM IC_{50} values) and potentially possess beneficial properties over orthosteric ligands.[17,21] Therefore, such allosteric ligands are of high relevance in drug discovery.[21−23]

Recent studies with orthosteric and allosteric ligands have demonstrated the capability of RORγt to bind both types of ligands simultaneously, even in a cooperative fashion.[17,24−26] These insights have inspired us to develop ligands that comprise a covalently linked orthosteric and allosteric pharmacophore to enable simultaneous targeting of both sites, also known as bitopic ligands.[27,28] Bitopic ligands were pioneered for G protein-coupled receptors (GPCRs).[27−30] Recently, the field of bitopic ligands has been expanded to other protein classes including kinases, e.g., mTor[31] and PKCα,[32] and a merged bitopic ligand for the nuclear receptor PPARγ.[33] These chemical biology studies have demonstrated that a dual targeting strategy is associated with several advantages over monovalent targeting strategies, including an increased affinity[30,34] or selectivity,[30,34−36] a bias in signaling pathway activation,[30,37] and reduced therapeutic resistance.[31]

Here, we describe the design, synthesis, and biochemical evaluation of three candidate bitopic ligands that comprise a covalently linked orthosteric and allosteric pharmacophore for RORγt (Figure 1), as the first linked bitopic ligands for NRs. Biochemical evaluation reveals that both **Bit-L15** and **Bit-L9** (linking both pharmacophores via a biamine linker with 15 and 9 PEG units) show bitopic RORγt binding characteristics, while **Bit-L4** (containing a short linker with 4 PEG units) does not show these characteristics, as anticipated by design. Most promisingly, **Bit-L15** has a significantly increased overall efficacy compared to its monovalent counterparts in both a biochemical and cellular context, approaching the activity of **MRL-871**. In addition, **Bit-L15** displays increased selectivity for RORγt over RORα and PPARγ compared to a cholesterol derivative and **MRL-871**, respectively. Combined, this study shows that bitopic modulation of RORγt might enable advantageous properties over classic monovalent NR targeting strategies, providing a framework for future studies investigating bitopic NR modulation.

https://dx.doi.org/10.1021/acschembio.0c00941
ACS Chem. Biol. 2021, 16, 510−519

Scheme 1. Synthesis of Bitopic Ligands[a,b]

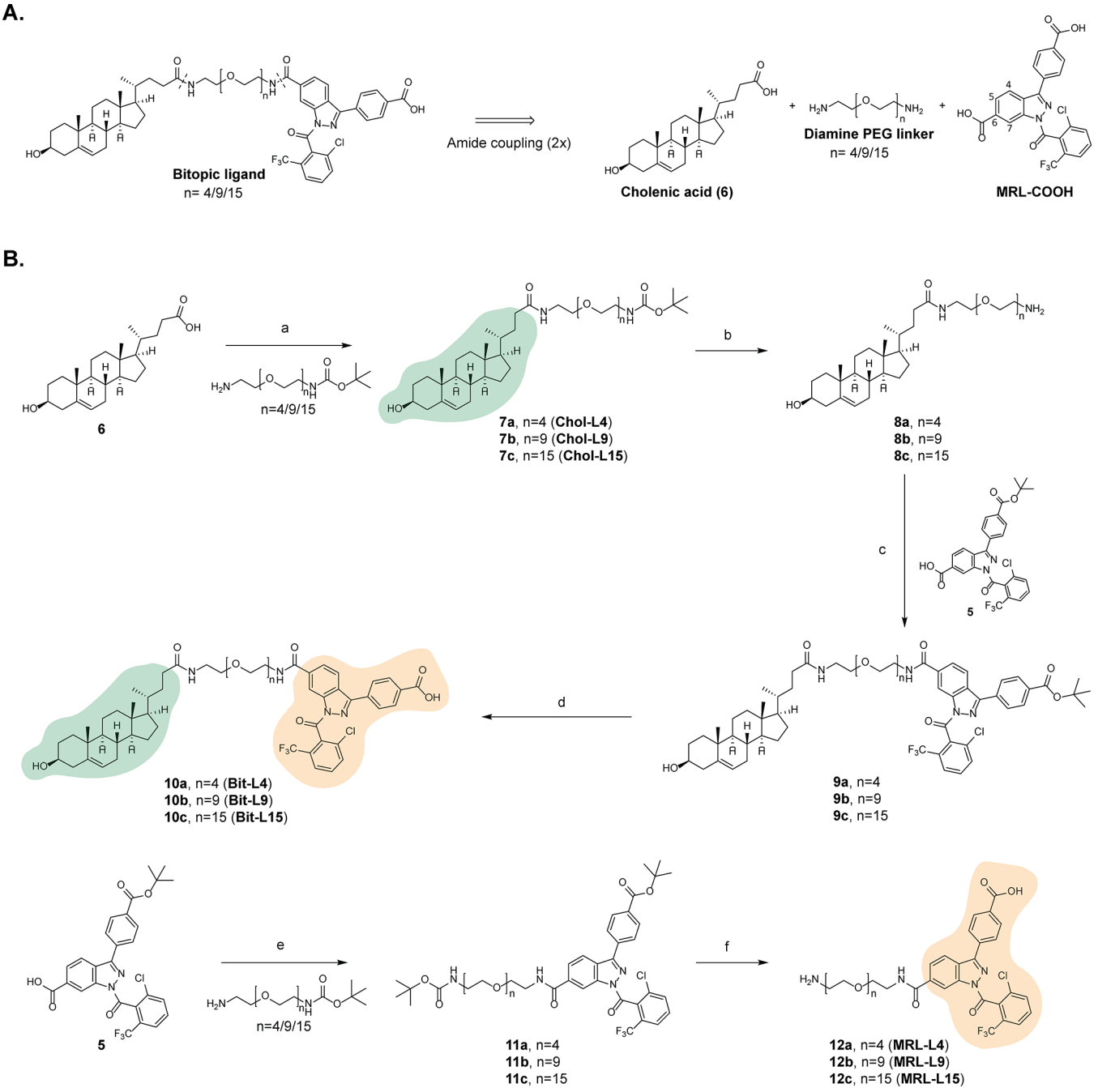

[a]Reagents and conditions: (a) DIPEA, HATU, DMF, RT, 3 h, 95% (**7a**), 86% (**7b**), 85% (**7c**); (b) (i) DCM/TFA/H_2O (65:30:5), RT, 3h; (ii) MeOH, 80 °C, O/N, quant. (**8a**, **8b**, **8c**); (c) DIPEA, HATU, DMF, RT, 3 h, 49% (**9a**), 56% (**9b**), 45% (**9c**); (d) (i) DCM/TFA/H_2O (65:30:5), RT, 3h; (ii) MeOH, 80 °C, O/N, quant. (**10a**, **10b**, **10c**); (e) DIPEA, HATU, DMF, RT, 3 h, 32% (**11a**), 51% (**11b**), 58% (**11c**); (f) DCM/TFA/H_2O (65:30:5), RT, 3h, quant. (**12a**, **12b**, **12c**). [b](A) Retrosynthesis of the designed bitopic ligands, via two amide coupling reactions between the carboxylic acid functionalities of cholenic acid and **MRL-COOH** and a biamine PEG linker (n = 4/9/15). (B) Synthesis of bitopic ligands **Bit-L4** (**10a**), **Bit-L9** (**10b**), and **Bit-L15** (**10c**) and monovalent ligands **Chol-L4** (**7a**), **Chol-L9** (**7b**), **Chol-L15** (**7c**) and **MRL-L4** (**12a**), **MRL-L9** (**12b**), and **MRL-L15** (**12c**).

2. RESULTS AND DISCUSSION

2.1. Design of the Bitopic RORγt Ligands. The first step in the design of a bitopic RORγt ligand was the identification of a suitable pharmacophore pair that could be used for linkage. Because of the concomitant binding observed for the orthosteric agonist cholesterol and allosteric inverse agonist **MRL-871** to RORγt,[24] these two pharmacophores were chosen for the bitopic ligand design. The crystal structure of RORγt with cholesterol and **MRL-871** (PDB: 6T4I)[24] (Figure 1) was used to devise a suitable strategy to link both ligands. The most promising linking strategy, in terms of space and retaining the key pharmacophore interactions with the LBD, was envisioned to be the coupling of the acyclic alkyl chain of cholesterol to the indazole core of **MRL-871**, yielding a bitopic ligand with the general structure shown in Figure 1.

https://dx.doi.org/10.1021/acschembio.0c00941
ACS Chem. Biol. 2021, 16, 510−519

Previous structure activity relationship (SAR) studies around **MRL-871** have shown that modifications at the C-6 position of the indazole scaffold are tolerated,[17,18] because this part of the molecule protrudes into an open channel in the cocrystal structure (Supporting Figure 1A). In previous studies, the C-6 position of **MRL-871** was functionalized with a carboxylic acid moiety (**MRL-COOH**, Scheme 1A), and various PEG linkers were attached to this handle via amide coupling chemistry (Supporting Figure 1B).[17] These modifications resulted in an affinity decrease of up to 30-fold relative to **MRL-871**, but the derivatives were still able to bind to the LBD of RORγt with IC_{50} values of 250 nM or lower.[17] Therefore, **MRL-COOH** (Scheme 1A) was used as entry for the attachment of a linker to the allosteric pharmacophore.

To keep the linking pathway between both sites as short as possible, the ideal position for linker attachment to the orthosteric pharmacophore is the alkyl tail of cholesterol (Figure 1), which is problematic due to the lack of a reactive handle at this position. Recently, Kallen and colleagues have published the crystal structure of cholenic acid (Scheme 1A), extended at its carboxylic acid position (Supporting Figure 1D).[38] Their work demonstrates that extended derivatives of cholenic acid maintain the ability to bind RORγt, and it highlights that the receptor is highly flexible in the H11 region (Supporting Figure 1C).[38] Although the extension induces a protein conformation that is incompatible with allosteric pocket formation due to displacement of H11, a less bulky and less rigid extension of cholenic acid is expected to disturb the agonistic protein conformation to a lesser extent, enabling the formation of the allosteric pocket. Therefore, cholenic acid was selected as entry for the attachment of a linker to the orthosteric pharmacophore.

The carboxylic acid moieties of **MRL-COOH** and cholenic acid allow the connection of both pharmacophores with a diamine linker via amide coupling chemistry to yield the desired bitopic ligands (Scheme 1A, Figure 1). In order to avoid nonspecific protein binding and to maintain flexibility and solubility, a polyethylene glycol (PEG) linker was used.[39] This type of linker is expected to maintain a high degree of conformational freedom upon bitopic binding to RORγt, which is beneficial from an entropic perspective. Additionally, PEG linkers have also been applied successfully in other bitopic ligands.[31] The distance between cholenic acid and the **MRL-871** derivative, following the linker path illustrated in Figure 1, was estimated via *in silico* measurements in the crystal structure to be 27.4 Å (Supporting Figure 2). A linker consisting of 9 PEG units (**Bit-L9**) (MM2 minimalized maximum nitrogen to nitrogen distance of the linker is 35.2 Å) was hypothesized to be just of adequate length to enable engagement with both sites. To verify this hypothesized mode, a linker consisting of 4 PEG units (**Bit-L4**), which is too short to span the distance around the protein, was also investigated (MM2 minimalized maximum nitrogen to nitrogen distance of the linker is 17.9 Å), as well as a ligand with a longer linker of 15 PEG units (**Bit-L15**) (MM2 minimalized maximum nitrogen to nitrogen distance of the linker is 56.9 Å).

2.2. Synthesis of the Ligands. The synthesis of the bitopic ligands was established via two amide coupling reactions with the three building blocks (Scheme 1): (1) the orthosteric ligand cholenic acid, (2) the diamine PEG linker (both commercially available), and (3) the allosteric ligand **MRL-COOH** (Scheme 1A). In order to prevent chemoselectivity issues during the synthesis, *tert*-butyloxycarbonyl (*t*-Boc) monoprotected biamine PEG linkers were used, and the **MRL-871** derivative was synthesized containing a *tert*-Butyl protected benzoic acid moiety.

The protected **MRL-COOH** derivative **5** was synthesized as described in literature,[17,18] with an overall yield of 39% (Supporting Scheme 1). The three bitopic ligands (**10a**, **10b**, **10c**) were synthesized via two amide coupling reactions, to couple the linker to both pharmacophores (Scheme 1B). While two strategies were tested for pharmacophore attachment (the orthosteric pharmacophore coupled first to the linker, followed by the allosteric pharmacophore, or vice versa), the strategy shown in Scheme 1B was deemed optimal; this is because a greater ease of purification resulted in overall higher yields.

First, the *t*-Boc monoprotected biamine PEG linkers were coupled to cholenic acid **6** via an amide coupling with DIPEA as base and HATU as coupling reagent, as described by Kallen et al.[38] The monovalent cholenic acid derivatives **7a** (**Chol-L4**), **7b** (**Chol-L9**), and **7c** (**Chol-L15**) were obtained in high yields. Subsequently, the linker was deprotected in a mixture of DCM:trifluoroacetic acid (TFA):water, resulting in the TFA-ester of the compounds (esterified at the alcohol moiety of cholenic acid). These were refluxed in methanol to hydrolyze the TFA ester to isolate compounds **8a**, **8b**, and **8c** in quantitative yields. Subsequently, these compounds were coupled to **5** via an amide coupling, resulting in the successful synthesis of **9a**, **9b**, and **9c**. The suboptimal yields at this stage are believed to be due to the formation of two unidentified side products, suspected to be related to compound **5**. After deprotection of the *tert*-Butyl protected acid of the **MRL-871** pharmacophore in quantitative yields, the desired bitopic ligands **10a**, **10b**, and **10c** were obtained, termed **Bit-L4**, **Bit-L9**, and **Bit-L15**.

In addition to the bitopic ligands, their monovalent counterparts were also synthesized to be used as a reference in biochemical evaluation. The monovalent orthosteric derivatives (**7a**, **7b**, and **7c**) were already obtained in the synthesis route toward the bitopic ligands (Scheme 1B). The monovalent allosteric derivatives **12a**, **12b**, and **12c** were synthesized from the **MRL-871** derivative **5** (Scheme 1B) via a similar amide coupling and deprotection strategy as described for the other ligands.

2.3. Biochemical Evaluation of the Binding Mode of the Bitopic Ligands. Various types of time-resolved FRET (TR-FRET) binding assays[40] were used to investigate the potency and binding mode of the bitopic ligands and monovalent counterparts. The cofactor recruitment TR-FRET assays are based on fluorescence emission occurring upon the FRET pairing of a d2-labeled cofactor with a terbium cryptate-labeled RORγt LBD (Figure 2E). In an orthogonal TR-FRET AlexaFluor-MRL recruitment assay (Figure 2F), an AlexaFluor647-labeled **MRL-871** probe is used (Supporting Figure 3) instead of the d2-labeled cofactor, enabling direct probing of allosteric site binding.

2.3.1. Binding Characteristics of Both Orthosteric and Allosteric Pharmacophores Are Retained. The binding behavior of the monovalent counterparts **MRL-L15** and **Chol-L15** (Scheme 1B, Figure 2G) was evaluated in a TR-FRET cofactor recruitment assay, to ensure that the attachment of a linker to either pharmacophore is not detrimental to ligand binding (Supporting Figure 4A,B). The allosteric monovalent counterpart **MRL-L15** shows a dose-dependent inverse agonistic behavior with an IC_{50} value of 0.26 ± 0.02 μM (Supporting Figure 4B), which is in the same range as

https://dx.doi.org/10.1021/acschembio.0c00941
ACS Chem. Biol. 2021, 16, 510−519

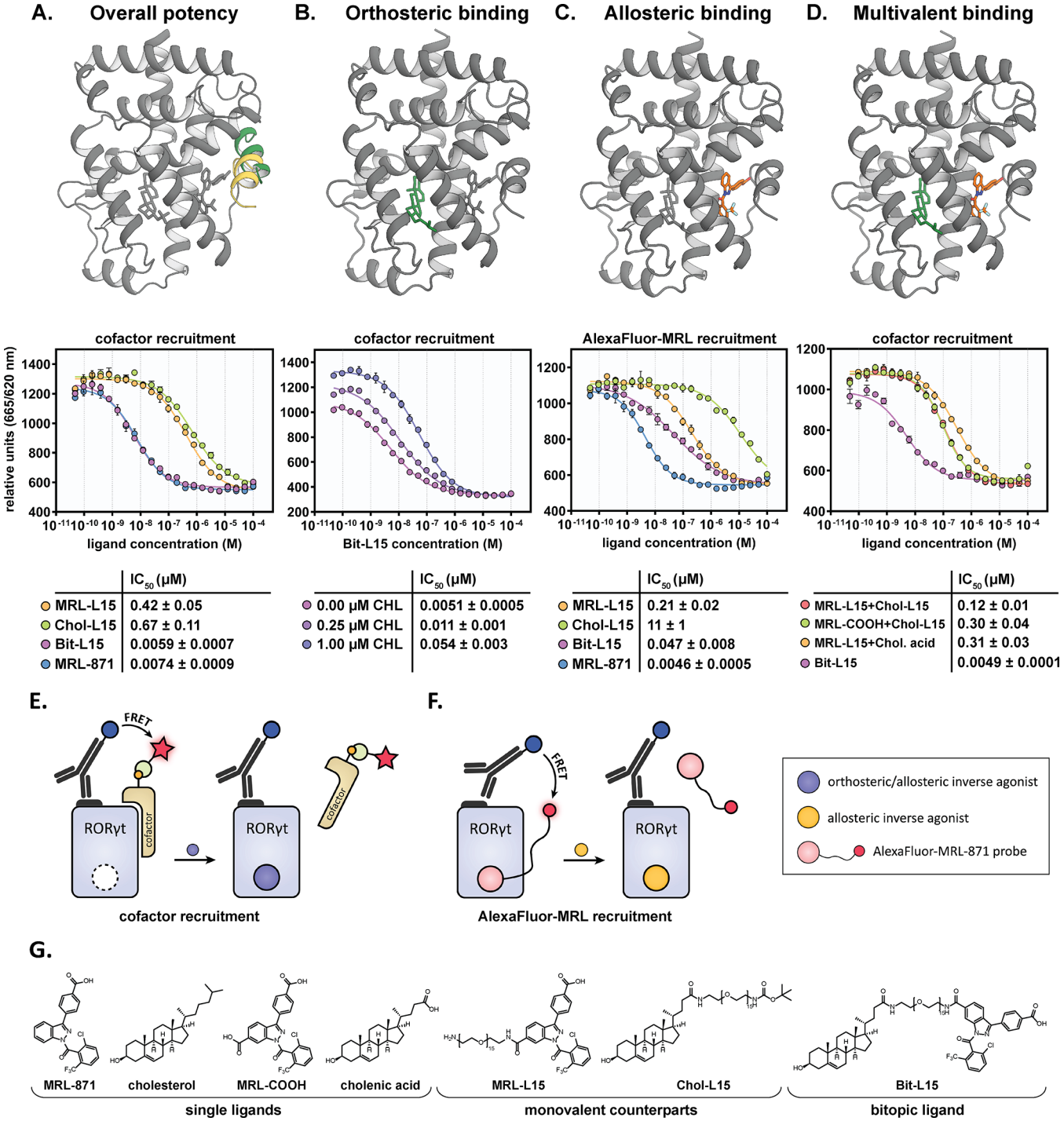

Figure 2. Overview of the different TR-FRET assay formats used to investigate the binding mode of the bitopic ligands: overall potency (A), orthosteric binding (B), allosteric binding (C), and multivalent binding (D). Below each assay schematic, the dose−response curves and an overview of the IC50 values are shown for the titration of single ligands, monovalent counterparts, and bitopic ligands to RORγt (cofactor recruitment-based assays (A, B, C) and AlexaFluor-MRL recruitment-based assay (D)). Abbreviations used: CHL = cholesterol, Chol. acid = cholenic acid. Data was recorded in two independent experiments, each recorded in triplicate (one representative data set shown). Error bars represent the SD of the mean. (E) Schematic representation of the TR-FRET coactivator recruitment assay. When RORγt is in its apo or agonist-bound state, the LBD binds the cofactor, resulting in FRET pairing of an anti-His terbium cryptate donor with the D2-labeled streptavidin acceptor. Inverse agonist binding results in cofactor displacement thus a lower FRET pairing. (F) Schematic representation of the TR-FRET AlexaFluor-MRL recruitment assay. When the probe binds to the RORγt LBD, there is FRET pairing between the anti-His terbium cryptate donor and the AlexaFluor647-MRL-871-labeled probe. Allosteric inverse agonist binding results in probe displacement thus a lower FRET pairing. (G) Chemical structures of single ligands (**MRL-871**, cholesterol, **MRL-COOH**, and cholenic acid), monovalent counterparts (**MRL-L15** and **Chol-L15**), and bitopic ligand (**Bit-L15**) used in the TR-FRET assays.

MRL-871-based probes containing a carboxamide modification at this position.[17,18] In the presence of cholesterol, no decrease in inhibitory potency of **MRL-L15** was observed, indicating an allosteric mode of binding (Supporting Figure

https://dx.doi.org/10.1021/acschembio.0c00941
ACS Chem. Biol. 2021, 16, 510−519

4B). In fact, even an increase in potency was observed for **MRL-L15** in the presence of cholesterol, indicating a cooperative behavior between both binding sites as has been observed previously (Supporting Figure 4B).[17,25,26] In contrast to the orthosteric agonist cholesterol,[1,16] the extended **Chol-L15** derivative is not compatible with coactivator recruitment and is thus an inverse agonist with an IC_{50} value of 0.54 ± 0.08 μM (Supporting Figure 4A), similar to the previously described extended cholenic acid derivative.[38] **Chol-L15** shows increasing IC_{50} values in the presence of cholesterol, indicating competition between the two ligands, verifying an orthosteric mode of binding (Supporting Figure 4A).

Investigation of the binding mode of the bitopic ligands was performed via four different TR-FRET assay formats, each probing a different aspect of binding (Figure 2A−D). Three different binding modes can be considered:[29] (1) a true bitopic mode of binding, concomitantly occupying both the orthosteric and allosteric site of the protein, (2) a flip-flop mode of binding, switching between a purely allosteric or purely orthosteric mode of binding (because both pockets cannot be occupied simultaneously), and (3) a mode of binding in which one bitopic ligand binds orthosterically and a second bitopic ligand binds allosterically, termed 2:1 binding (ligand:protein stoichiometry). Although a true bitopic and a flip-flop mode of binding can be difficult to distinguish experimentally, the latter is not expected in this case, because this mode is only worthwhile to consider in the case of small size pharmacophores with low binding affinities, instead of voluminous high affinity ligands that have a fixed binding topography, as is the case here.[29,41] Based on their design, a true bitopic binding mode is expected for **Bit-L9** and **Bit-L15**, while a monovalent or 2:1 mode of binding is expected for **Bit-L4** (with the latter being less likely due to aforementioned reasons).

2.3.2. Linking Both Pharmacophores Increases Potency of Bit-L15 for RORγt Compared to Monovalent Counterparts. The three bitopic ligands and their monovalent counterparts were examined in a TR-FRET coactivator recruitment assay to investigate the effect of the different linkages of both pharmacophores on the inhibition of cofactor recruitment (Figure 2A). The results for the PEG-15 ligands demonstrate that the monovalent counterparts **MRL-L15** and **Chol-L15** show IC_{50} values of 0.42 ± 0.05 and 0.67 ± 0.11 μM, respectively, whereas the bitopic ligand **Bit-L15** shows a significantly higher potency with an IC_{50} value of 0.0059 ± 0.0007 μM, comparable to the highly potent allosteric ligand **MRL-871** (Figure 2A). These results demonstrate that the linkage of the allosteric **MRL-871** and the orthosteric cholenic acid pharmacophore via a PEG-15 linker is beneficial for the overall potency of the ligand. For the second bitopic ligand with a PEG-9 linker (**Bit-L9**), a similar behavior was observed, although the overall potency of this bitopic ligand was slightly lower than that for **Bit-L15** (Supporting Figure 5A). In stark contrast, the bitopic ligand **Bit-L4** with the shorter PEG-4 linker does not show a significant increase in potency relative to the monovalent counterparts. Instead, it shows an IC_{50} value comparable to **MRL-L4** (the highest affinity monovalent counterpart) (Supporting Figure 5B), providing evidence that the bitopic binding mode cannot be established with this short linker length.

In order to further validate these results, the TR-FRET coactivator recruitment assay was performed with a modified RORγt LBD in which the orthosteric site was blocked via ligation of a chemical probe to a native cysteine residue (Cys320) in the orthosteric ligand binding pocket (Supporting Figure 6A).[42] This probe prevents orthosteric ligands from binding to RORγt, while the allosteric binding site remains accessible for binding of allosteric ligands. As expected, when the orthosteric site is not available for binding, **Bit-L15** and **Bit-L9** show IC_{50} values in the same ballpark as their monovalent allosteric counterparts **MRL-L15** and **MRL-L9** (Supporting Figure 6B,C). In general, the absolute IC_{50} values are lower than in the regular coactivator recruitment assay, due to cooperativity between the covalent orthosteric probe and the allosteric binding ligands.[17,25,26] In contrast, **Bit-L4** shows a lower potency than that of its monovalent allosteric counterpart **MRL-L4** (Supporting Figure 6D). This lower potency is presumably due to unfavorable interactions or steric clashes between the protein and the unbound orthosteric cholenic acid moiety upon binding of **Bit-L4** to the allosteric site (caused by the shorter linker), decreasing the allosteric site affinity relative to **MRL-L4**. Combined, these results demonstrate that the increase in overall potency of **Bit-L15** and **Bit-L9** relative to **MRL-L15** and **MRL-L9** in the coactivator recruitment assay with the native RORγt LBD is due to concomitant engagement of both sites.

2.3.3. Bit-L15 Competes with Cholesterol for Orthosteric Site Binding. In order to probe the importance of the orthosteric site in binding of the bitopic ligands in more detail, the TR-FRET coactivator recruitment assay was performed in the absence and presence of the orthosteric ligand cholesterol (CHL) (Figure 2B). The results in Figure 2B show that, in the absence of cholesterol, **Bit-L15** exhibits a dose-dependent inverse agonistic character, in agreement with the previous assay. However, when the same titration is performed in the presence of a fixed concentration of cholesterol, the IC_{50} values decrease (shift of the curves to the right) with increasing cholesterol concentration (Figure 2B). This shift in IC_{50} values demonstrates a competitive character between **Bit-L15** and cholesterol, indicating once more that orthosteric binding is involved in the mode of action of **Bit-L15**. A similar increase in IC_{50} values is observed for **Bit-L9** and **Bit-L4** (Supporting Figure 7A,B), confirming that these bitopic ligands feature an orthosteric component in their binding mode as well.

Upon closer examination, a trend can be observed between the linker length of the bitopic ligands and the degree of competition with cholesterol. As can be seen in Supporting Figure 7C, the bitopic ligands with a longer linker length show a higher fold decrease in potency in the presence of cholesterol compared to ligands with a shorter linker length, indicating that a bitopic ligand with a longer linker becomes relatively more susceptible to competition with cholesterol. This suggests that **Bit-L15** gains more of its overall potency from the orthosteric site compared to **Bit-L9** and **Bit-L4**. The low sensitivity of **Bit-L4** to cholesterol competition is evidence that **Bit-L4** binds mainly via the allosteric pocket.

2.3.4. Bit-L15 Shows Increased Competition with an Allosteric Probe Compared to the Monovalent MRL-L15. The orthogonal TR-FRET AlexaFluor-MRL recruitment assay (Figure 2F) was used to investigate the allosteric binding behavior of the bitopic ligands (Figure 2C). **MRL-L15** demonstrates a clear dose−response curve, displacing the AlexaFluor-**MRL-871** probe with an IC_{50} value of 0.21 ± 0.02 μM. In contrast, **Chol-L15** shows the typical behavior for an orthosteric ligand with an IC_{50} value >10 μM.[25] **Bit-L15** displaces the allosteric probe with an IC_{50} value of 0.047 ±

https://dx.doi.org/10.1021/acschembio.0c00941
ACS Chem. Biol. 2021, 16, 510−519

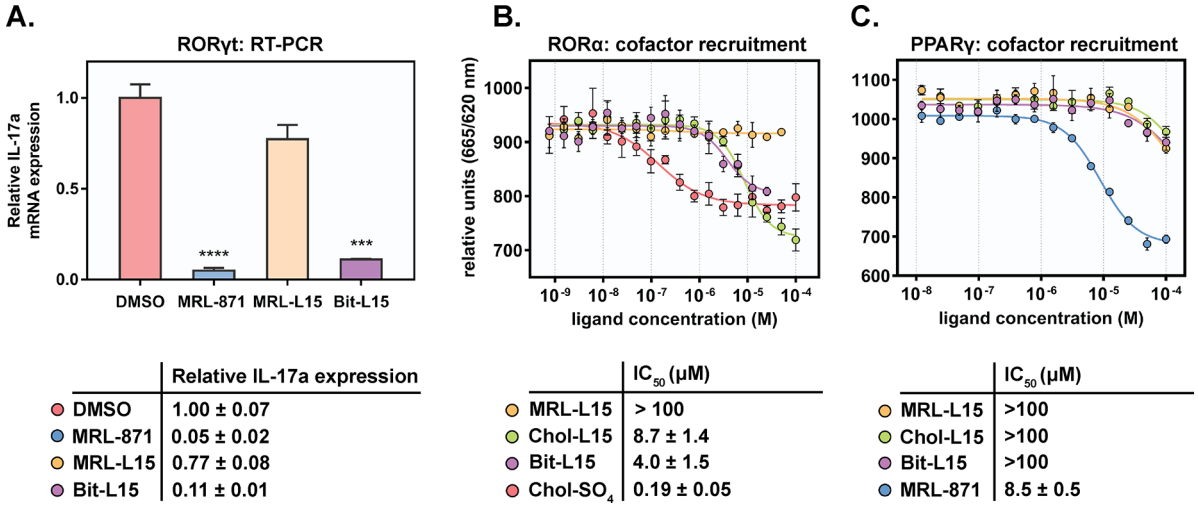

	Relative IL-17a expression
DMSO	1.00 ± 0.07
MRL-871	0.05 ± 0.02
MRL-L15	0.77 ± 0.08
Bit-L15	0.11 ± 0.01

	IC_{50} (μM)
MRL-L15	> 100
Chol-L15	8.7 ± 1.4
Bit-L15	4.0 ± 1.5
Chol-SO_4	0.19 ± 0.05

	IC_{50} (μM)
MRL-L15	>100
Chol-L15	>100
Bit-L15	>100
MRL-871	8.5 ± 0.5

Figure 3. (A) IL-17a mRNA expression in EL4 cells treated with ligands **MRL-871**, **MRL-L15**, **Bit-L15** (10 μM, 24 h), or DMSO. The level of IL-17a expression was normalized to that of GAPDH expression. All data are expressed as the mean ± s.d. (standard deviation) (n = 3). The relative gene expression was calculated by the $2^{-\Delta\Delta Ct}$ (Livak) method using the DMSO control as calibrator. Statistical analysis was performed using a one-way analysis of variance compared against the DMSO control following Dunnett post hoc test; ***P < 0.001 and ****P < 0.0001. (B) Dose–response curves of TR-FRET assays by titration of **MRL-L15**, **Chol-L15**, **Bit-L15**, and **Chol-SO_4** to RORα, including an overview of the IC_{50} values (the last 2 data points for **Bit-L15** and last data point for **MRL-L15** are not shown because of solubility issues at high concentrations). (C) Dose–response curves of TR-FRET assays by titration of **MRL-871**, **MRL-L15**, **Chol-L15**, and **Bit-L15** to PPARγ, including an overview of the IC_{50} values.

0.008 μM, confirming allosteric site binding. Relative to **MRL-L15**, the potency is increased 4.5-fold, which can be explained by an enhanced local concentration of the allosteric component due to concomitant binding of **Bit-L15** to the orthosteric site (tethering effect), again validating the bitopic binding mode of **Bit-L15**.

Bit-L9 and its monovalent counterparts show a comparable behavior to **Bit-L15** (Supporting Figure 8A), with **Bit-L9** featuring a 2.7-fold increase in potency compared to the monovalent **MRL-L9** (IC_{50} = 0.058 ± 0.007 vs 0.16 ± 0.02 μM, respectively). For **Bit-L4**, allosteric site binding is observed as well, however without a tethering effect. In contrast to **Bit-L15** and **Bit-L9**, **Bit-L4** is approximately 8-fold less potent than its monovalent allosteric counterpart **MRL-L4** (Supporting Figure 8B). This demonstrates that the coupling of the orthosteric pharmacophore to **MRL-L4** weakens the affinity for the allosteric site, presumably due to a steric clash as discussed in the cofactor recruitment assay and is in agreement with the hypothesis that **Bit-L4** cannot bind both sites simultaneously. Combined, **Bit-L15** and **Bit-L9** demonstrate an increased potency relative to their allosteric monovalent counterparts, ascribed to a tethering effect from the orthosteric binding pharmacophore.

2.3.5. Bit-L15 Exhibits Increased Potency Relative to Coincubated Monovalent Counterparts. With the binding to both the orthosteric and allosteric site confirmed, the affinity of the bitopic ligands was compared to their simultaneously incubated monovalent counterparts in a TR-FRET coactivator recruitment assay (Figure 2D) to probe the presence of a multivalent effect (i.e., an increased affinity compared to equimolar amounts of coincubated unlinked counterparts).[36]

As shown in Figure 2D, **Bit-L15** has a higher overall affinity in the coactivator recruitment assay compared to equimolar amounts of coincubated monovalent counterparts (different combinations of coincubated monovalent counterparts were examined). Depending on the combination of coincubated ligands, a 23- to 63-fold higher affinity can be observed for **Bit-L15**. This multivalent effect provides convincing evidence for a true bitopic binding mode to the RORγt LBD.[36] A potential 2:1 binding mode can be excluded based on these results, because in this binding scenario, **Bit-L15** would have been equally potent as the coincubated monovalent ligands with linker.

Similarly, **Bit-L9** also shows a multivalent effect (Supporting Figure 9A), although with a slightly lower magnitude (5- to 11-fold increase in potency compared to the coincubated ligands). In contrast, the potency of **Bit-L4** is similar to the coincubated monovalent counterparts and therefore lacks a multivalent effect, in agreement with the hypothesis that this ligand cannot bind both pockets simultaneously due to inadequate linker length (Supporting Figure 9B). The results of **Bit-L4** suggest a 2:1 binding stoichiometry, with one **Bit-L4** ligand binding orthosterically and another one binding allosterically.

2.4. Bit-L15 Inhibits IL-17a Expression in EL4 Cells. RORγt is the master transcription factor in Th17 cell differentiation and promotes IL-17a production. Therefore, the cellular activity of **Bit-L15** was determined by measuring the reduction of IL-17a mRNA expression levels by quantitative reverse transcriptase PCR (RT-PCR), to provide a first indication on the efficacy of **Bit-L15** in a cellular context. The inhibition of IL-17a mRNA expression was measured in EL4 cells, a murine lymphoblast cell line that constitutively expresses RORγt. The EL4 cells were treated with 10 μM **MRL-871**, **MRL-L15**, and **Bit-L15** for 24 h before the mRNA levels were measured (Figure 3A). Both **MRL-871** and **Bit-L15** are active and potent in a cellular context. **MRL-871** significantly reduced IL-17a mRNA expression 21-fold, in line with previous reports.[25] **Bit-L15** led to a significant decrease in IL-17a expression as well (9-fold), demonstrating the desired effect not only in a direct biochemical assay but also in a cellular context despite its nondruglike chemical structure (high molecular weight, long linker, and hydrophobic cholenic acid moiety). In contrast, **MRL-L15** shows only a minor reduction of IL-17a mRNA expression (1.3-fold) compared to

https://dx.doi.org/10.1021/acschembio.0c00941
ACS Chem. Biol. 2021, 16, 510–519

Bit-L15, which shows that the coupling of the cholesterol pharmacophore to the allosteric pharmacophore results in a significantly higher response than for the monovalent allosteric counterpart alone. The results are in agreement with the results from the TR-FRET coactivator recruitment assays, where **MRL-871** and **Bit-L15** show a similar overall affinity for RORγt, while **MRL-L15** is less potent (IC_{50} value of 0.0059 μM for **Bit-L15** vs 0.42 μM for **MRL-L15**, Figure 2A). However, the increase in cellular efficacy of **Bit-L15** relative to **MRL-L15** might also be caused by active cellular uptake facilitated by the attachment of the cholesterol pharmacophore to **MRL-871**.[43]

2.5. Bit-L15 is Selective for RORγt over RORα and PPARγ. In addition to an increased overall potency, the second major feature of a bitopic ligand over its monovalent orthosteric and allosteric ligands is an increased selectivity for its target by concomitant engagement of two sites.[29,41] Cholesterol and its derivatives are known to not only bind to RORγt but also to have cross-reactivity toward RORα with high affinities.[1] In order to investigate the cross-reactivity of **Bit-L15** on RORα, a TR-FRET cofactor recruitment assay was performed. Whereas sulfated cholesterol (Chol-SO_4) shows a clear activity toward RORα with an IC_{50} value of 0.19 ± 0.05 μM, **Bit-L15** was more than 20 times less active in recruiting coactivator (IC_{50} value of 4.0 ± 1.5 μM) (Figure 3B). These results show that **Bit-L15** exhibits some off-target activity on RORα but with a significant decrease in potency compared to that of sulfated cholesterol.

Furthermore, it has been demonstrated that **MRL-871** and its derivatives possess off-target effects against the peroxisome proliferator-activated receptor γ (PPARγ).[17,20] In order to probe the cross-reactivity of the bitopic ligands on PPARγ, a similar TR-FRET assay was performed with **Bit-L15** (Figure 3C). In agreement with literature,[17,25] **MRL-871** shows an IC_{50} value of 8.5 ± 0.5 μM (vs 0.0074 ± 0.0009 μM for RORγt), whereas **Bit-L15** shows an IC50 value >100 μM (vs 0.0059 ± 0.0007 μM for RORγt), demonstrating that **Bit-L15** is considerably more selective for RORγt than **MRL-871**. Additionally, a competition experiment was performed with the ligands and a known PPARγ ligand (tesaglitazar).[44] The data shows that the competition between **MRL-871** and tesaglitazar is considerably higher than between **Bit-L15** and tesaglitazar (respectively, 84 vs 1.3 times maximal increase in IC_{50} values), again indicating a higher selectivity of **Bit-L15** for PPARγ compared to **MRL-871** (Supporting Figure 10). These data clearly demonstrate how bitopic targeting can enhance the selectivity for a target.

3. CONCLUSION

The recent discovery of the simultaneous binding of an orthosteric and allosteric ligand to the LBD of RORγt inspired the design of bitopic RORγt ligands that, in theory, could concomitantly occupy both the orthosteric and allosteric site of the protein. Compared to monovalent targeting strategies, successful bitopic targeting of various classes of proteins has been associated with advantages including an increased overall affinity or a higher selectivity profile. Bitopic targeting of RORγt might therefore yield desirable molecular pharmacological properties. We report the design, synthesis, and biochemical and cellular evaluation of three candidate bitopic ligands **Bit-L15**, **Bit-L9**, and **Bit-L4**, connecting an orthosteric and allosteric RORγt pharmacophore via a PEG linker that varies in linker length from four to 15 PEG units.

A combination of TR-FRET assays was performed to probe different aspects of the mode of binding for all three bitopic ligands. A strong dependence of the overall affinity on linker length was observed, with both **Bit-L15** and **Bit-L9** showing an increase in potency relative to their individual monovalent counterparts, while **Bit-L4** showed a comparable potency to that of the allosteric monovalent counterpart. **Bit-L15** was the most potent of the bitopic ligands, matching the low nanomolar affinity of the allosteric inverse agonist **MRL-871**. Several follow-up assays confirmed that **Bit-L15** and **Bit-L9** bind both in the orthosteric and allosteric site simultaneously. Comparison of the bitopic compounds with equimolar amounts of coincubated monovalent counterparts demonstrated that, for **Bit-L15** and **Bit-L9**, a more than additive effect of both monovalent counterparts exists. For **Bit-L4**, such a multivalent effect was, as expected, not observed. Combined, the TR-FRET data for **Bit-L15** reveal a bitopic binding mode and a multivalent character, illustrated by its higher potency compared to the (coincubated) monovalent pharmacophores. **Bit-L9** also binds bitopically, but with a lower overall potency and less multivalent character. This could be related to an entropic penalty caused by tension in the shorter linker, upon bitopic binding. **Bit-L4** lacks the typical characteristics of bitopic binding and most probably binds via a 2:1 binding mode.

The most potent bitopic compound, **Bit-L15**, was also evaluated in a cellular setting to explore functional efficacy. Indeed, **Bit-L15** showed a clear reduction of IL-17a levels, approaching the activity of **MRL-871**. Finally, the selectivity of **Bit-L15** was investigated in TR-FRET assays with PPARγ and RORα. **Bit-L15** was found to be more than 20 times less active for RORα than a sulfated cholesterol derivative and displays hardly any activity for PPARγ (IC_{50} > 100 μM) compared to **MRL-871**, clearly demonstrating the enhancement of selectivity for RORγt via a dual targeting strategy.

In conclusion, we have rationally designed three candidate bitopic RORγt ligands, **Bit-L15**, **Bit-L9**, and **Bit-L4**. Biochemical evaluation via various TR-FRET assays provides strong evidence that **Bit-L15** and **Bit-L9** bind RORγt in a bitopic manner, with **Bit-L15** showing the most promising characteristics. Furthermore, bitopic targeting results in an increased target selectivity while retaining overall efficacy in both a biochemical and cellular context. Bitopic NR modulation thus positions itself as a highly promising alternative to monovalent strategies, as chemical biology tool compounds, or maybe even toward alternative NR targeting strategies. Future studies focusing on the drug likeness of the bitopic RORγt modulators (e.g., pharmacokinetic properties, cytotoxicity studies, and elaboration on the selectivity profile) are required to determine the relevance of these ligands beyond a chemical biology point of view.

■ ASSOCIATED CONTENT

Supporting Information

The Supporting Information is available free of charge at https://pubs.acs.org/doi/10.1021/acschembio.0c00941.

Additional figures, synthetic procedures, compound characterization, detailed description of methods concerning protein expression, in silico measurements, and biochemical assays (PDF)

Compound characterization checklist (XLS)

https://dx.doi.org/10.1021/acschembio.0c00941
ACS Chem. Biol. 2021, 16, 510−519

AUTHOR INFORMATION

Corresponding Author

Luc Brunsveld − *Laboratory of Chemical Biology, Department of Biomedical Engineering and Institute for Complex Molecular Systems, Technische Universiteit Eindhoven, Eindhoven 5612, AZ, The Netherlands;* orcid.org/0000-0001-5675-511X; Email: l.brunsveld@tue.nl

Authors

Femke A. Meijer − *Laboratory of Chemical Biology, Department of Biomedical Engineering and Institute for Complex Molecular Systems, Technische Universiteit Eindhoven, Eindhoven 5612, AZ, The Netherlands;* orcid.org/0000-0003-4412-9968

Guido J.M. Oerlemans − *Laboratory of Chemical Biology, Department of Biomedical Engineering and Institute for Complex Molecular Systems, Technische Universiteit Eindhoven, Eindhoven 5612, AZ, The Netherlands;* orcid.org/0000-0001-7562-2654

Complete contact information is available at: https://pubs.acs.org/10.1021/acschembio.0c00941

Author Contributions

†F.A.M. and G.J.M.O. contributed equally to this work. The manuscript was written through contributions of all authors. G.J.M.O. performed synthesis, and G.J.M.O. and F.A.M. performed biochemical studies; F.A.M., G.J.M.O., and L.B. designed the studies. All authors have given approval to the final version of the manuscript.

Funding

This work was supported by The Netherlands Organization for Scientific Research through Gravity program 024.001.035 and VICI grant 016.150.366.

Notes

The authors declare no competing financial interest.

ACKNOWLEDGMENTS

We thank M. van den Oetelaar and I. Leijten−van de Gevel for expression of the RORγt protein, A. Koops for expression of the PPARγ protein, J. van Dongen for performing HRMS measurements, and R. de Vries for his efforts in crystallography experiments.

ABBREVIATIONS

CHL, cholesterol; GPCR, G-protein coupled receptor; H12, helix 12; IPTG, isopropyl-b-d-thiogalactoside; LBD, ligand binding domain; LC-MS, liquid chromatography−mass spectrometry; NR, Nuclear Receptor; PEG, polyethylene glycol; Q-ToF, quadrupole time-of-flight; RORγt, retinoic acid receptor-related orphan receptor γ t; RT-PCR, reverse transcriptase PCR; SAR, structure activity relationship; *t*-Boc, *tert*-butyloxycarbonyl; TFA, trifluoroacetic acid; Th17, T helper 17; TR-FRET, time-resolved FRET

REFERENCES

(1) Solt, L. A., and Burris, T. P. (2012) Action of RORs and their ligands in (patho)physiology. *Trends Endocrinol. Metab. 23*, 619−627.

(2) Ivanov, I. I., et al. (2006) The Orphan Nuclear Receptor RORγt Directs the Differentiation Program of Proinflammatory IL-17+ T Helper Cells. *Cell 126*, 1121−1133.

(3) Manel, N., Unutmaz, D., and Littman, D. R. (2008) The differentiation of human TH-17 cells requires transforming growth factor-β and induction of the nuclear receptor RORγt. *Nat. Immunol. 9*, 641−649.

(4) Miossec, P., and Kolls, J. K. (2012) Targeting IL-17 and TH17 cells in chronic inflammation. *Nat. Rev. Drug Discovery 11*, 763−776.

(5) Yang, J., Sundrud, M. S., Skepner, J., and Yamagata, T. (2014) Targeting Th17 cells in autoimmune diseases. *Trends Pharmacol. Sci. 35*, 493−500.

(6) Burkett, P. R., and Kuchroo, V. K. (2016) IL-17 Blockade in Psoriasis. *Cell 167*, 1669.

(7) Lock, C., et al. (2002) Gene-microarray analysis of multiple sclerosis lesions yields new targets validated in autoimmune encephalomyelitis. *Nat. Med. 8*, 500−508.

(8) Isono, F., Fujita-Sato, S., and Ito, S. (2014) Inhibiting RORγt/Th17 axis for autoimmune disorders. *Drug Discovery Today 19*, 1205−1211.

(9) Fauber, B. P., and Magnuson, S. (2014) Modulators of the nuclear receptor retinoic acid receptor-related orphan receptor-γ (RORγ or RORc). *J. Med. Chem. 57*, 5871−5792.

(10) Bronner, S. M., Zbieg, J. R., and Crawford, J. J. (2017) RORgamma antagonists and inverse agonists: a patent review. *Expert Opin. Ther. Pat. 27*, 101−112.

(11) Cyr, P., Bronner, S. M., and Crawford, J. J. (2016) Recent progress on nuclear receptor RORγ modulators. *Bioorg. Med. Chem. Lett. 26*, 4387−4393.

(12) Huh, J. R., et al. (2013) Identification of Potent and Selective Diphenylpropanamide RORγ Inhibitors. *ACS Med. Chem. Lett. 4*, 79−84.

(13) Kotoku, M., et al. (2019) Discovery of Second Generation RORγ Inhibitors Composed of an Azole Scaffold. *J. Med. Chem. 62*, 2837−2842.

(14) Duan, J. J.-W., et al. (2019) Structure-based Discovery of Phenyl (3-Phenylpyrrolidin-3-yl)sulfones as Selective, Orally Active RORγt Inverse Agonists. *ACS Med. Chem. Lett. 10*, 367−373.

(15) Li, X., et al. (2017) Structural studies unravel the active conformation of apo RORγt nuclear receptor and a common inverse agonism of two diverse classes of RORγt inhibitors. *J. Biol. Chem. 292*, 11618−11630.

(16) Hu, X., et al. (2015) Sterol metabolism controls TH17 differentiation by generating endogenous RORγ agonists. *Nat. Chem. Biol. 11*, 141−147.

(17) Scheepstra, M., et al. (2015) Identification of an allosteric binding site for RORγt inhibition. *Nat. Commun. 6*, No. e8833.

(18) Karstens, W. F. J., et al. (2012) RORgammaT Inhibitors, PCT Int. Appl. WO 2012/106995.

(19) Ouvry, G., et al. (2016) Discovery of phenoxyindazoles and phenylthioindazoles as RORγ inverse agonists. *Bioorg. Med. Chem. Lett. 26*, 5802−5808.

(20) Fauber, B. P., et al. (2015) Discovery of imidazo[1,5-a]pyridines and -pyrimidines as potent and selective RORc inverse agonists. *Bioorg. Med. Chem. Lett. 25*, 2907−2912.

(21) Meijer, F. A., Leijten-Van de Gevel, I. A., de Vries, R. M. J. M., and Brunsveld, L. (2019) Allosteric small molecule modulators of nuclear receptors. *Mol. Cell. Endocrinol. 485*, 20−34.

(22) Tice, C. M., and Zheng, Y.-J. (2016) Non-canonical modulators of nuclear receptors. *Bioorg. Med. Chem. Lett. 26*, 4157−4164.

(23) Moore, T. W., Mayne, C. G., and Katzenellenbogen, J. a. (2010) Minireview: Not picking pockets: nuclear receptor alternate-site modulators (NRAMs). *Mol. Endocrinol. 24*, 683−695.

(24) de Vries, R. M. J. M., Meijer, F. A., Doveston, R. G., Leijten-Van de Gevel, I. A., and Brunsveld, L. (2021) Cooperativity between the Orthosteric and Allosteric Ligand Binding Sites of RORγt. *Proc. Natl. Acad. Sci. U. S. A. 118*, No. e2021287118.

(25) Meijer, F. A., et al. (2020) Ligand-Based Design of Allosteric Retinoic Acid Receptor-Related Orphan Receptor γt (RORγt) Inverse Agonists. *J. Med. Chem. 63*, 241−259.

(26) de Vries, R. M. J. M., Meijer, F. A., Doveston, R. G., and Brunsveld, L. (2020) Elucidation of an Allosteric Mode of Action for a Thienopyrazole RORγt Inverse Agonist. *ChemMedChem 15*, 561−565.

(27) Fronik, P., Gaiser, B. I., and Sejer Pedersen, D. (2017) Bitopic Ligands and Metastable Binding Sites: Opportunities for G Protein-Coupled Receptor (GPCR) Medicinal Chemistry. *J. Med. Chem. 60*, 4126−4134.
(28) Newman, A. H., Battiti, F. O., Bonifazi, A., and Philip, S. (2020) Portoghese Medicinal Chemistry Lectureship: Designing Bivalent or Bitopic Molecules for G-Protein Coupled Receptors. The Whole Is Greater Than the Sum of Its Parts. *J. Med. Chem. 63*, 1779−1797.
(29) Lane, J. R., Sexton, P. M., and Christopoulos, A. (2013) Bridging the gap: bitopic ligands of G-protein-coupled receptors. *Trends Pharmacol. Sci. 34*, 59−66.
(30) Valant, C., Sexton, P. M., and Christopoulos, A. (2009) Orthosteric/allosteric bitopic ligands: going hybrid at GPCRs. *Mol. Interventions 9*, 125−135.
(31) Rodrik-Outmezguine, V. S., et al. (2016) Overcoming mTOR resistance mutations with a new-generation mTOR inhibitor. *Nature 534*, 272−276.
(32) Ma, N., et al. (2018) Bitopic Inhibition of ATP and Substrate Binding in Ser/Thr Kinases through a Conserved Allosteric Mechanism. *Biochemistry 57*, 6387−6390.
(33) Brust, R., et al. (2017) Modification of the Orthosteric PPARγ Covalent Antagonist Scaffold Yields an Improved Dual-Site Allosteric Inhibitor. *ACS Chem. Biol. 12*, 969−978.
(34) Battiti, F. O., et al. (2019) The Significance of Chirality in Drug Design and Synthesis of Bitopic Ligands as D3 Receptor (D3R) Selective Agonists. *J. Med. Chem. 62*, 6287−6314.
(35) Morales, P., et al. (2020) Discovery of Homobivalent Bitopic Ligands of the Cannabinoid CB2 Receptor. *Chem. - Eur. J. 26*, 15839−15842.
(36) Steinfeld, T., Mammen, M., Smith, J. A. M., Wilson, R. D., and Jasper, J. R. (2007) A Novel Multivalent Ligand That Bridges the Allosteric and Orthosteric Binding Sites of the M2Muscarinic Receptor. *Mol. Pharmacol. 72*, 291−302.
(37) Egyed, A., et al. (2020) Controlling receptor function from the extracellular vestibule of G-protein coupled receptors. *Chem. Commun. (Cambridge, U. K.) 56*, 14167−14170.
(38) Kallen, J., et al. (2017) Structural States of RORgammat: X-ray Elucidation of Molecular Mechanisms and Binding Interactions for Natural and Synthetic Compounds. *ChemMedChem 12*, 1014−1021.
(39) Bastings, M. M. C., de Greef, T. F. A., van Dongen, J. L. J., Merkx, M., and Meijer, E. W. (2010) Macrocyclization of enzyme-based supramolecular polymers. *Chem. Sci. 1*, 79−88.
(40) Degorce, F. (2009) HTRF: A Technology Tailored for Drug Discovery - A Review of Theoretical Aspects and Recent Applications. *Curr. Chem. Genomics 3*, 22−32.
(41) Mohr, K., et al. (2010) Rational design of dualsteric GPCR ligands: quests and promise. *Br. J. Pharmacol. 159*, 997−1008.
(42) Leesnitzer, L. M., et al. (2002) Functional Consequences of Cysteine Modification in the Ligand Binding Sites of Peroxisome Proliferator Activated Receptors by GW9662. *Biochemistry 41*, 6640−6650.
(43) Petrova, N. S., et al. (2012) Carrier-free cellular uptake and the gene-silencing activity of the lipophilic siRNAs is strongly affected by the length of the linker between siRNA and lipophilic group. *Nucleic Acids Res. 40*, 2330−2344.
(44) Chira, E. C., et al. (2007) Tesaglitazar, a dual peroxisome proliferator-activated receptor alpha/gamma agonist, reduces atherosclerosis in female low density lipoprotein receptor deficient mice. *Atherosclerosis 195*, 100−109.

https://dx.doi.org/10.1021/acschembio.0c00941
ACS Chem. Biol. 2021, 16, 510−519